Desalination and Water Treatment
www.deswater.com
doi: 10.1080/19443994.2012.749325

51 (2013) 3445–3453
April

Taylor & Francis
Taylor & Francis Group

CFD modeling of hydrophobic pervaporation process: ethanol/water separation

Mostafa Keshavarz Moraveji[a]*, Ahmadreza Raisi[b], Seyede Maryam Hosseini[a], Elahe Esmaeeli[a], Gholamreza Pazuki[b]

[a]*Department of Chemical Engineering, Arak University, Arak 38156-8-8349, Iran*
Tel. +98 9363098063; Fax: +98 861 4173450; email: m-moraveji@araku.ac.ir
[b]*Department of Chemical Engineering, Amirkabir University of Technology (Tehran Polytechnic), Tehran, Iran*

Received 6 March 2012; Accepted 6 September 2012

ABSTRACT

The computational fluid dynamics (CFD) approach was employed to model the pervaporation separation of ethanol from its aqueous solutions with polydimethylsiloxane (PDMS) membrane. The proposed CFD model was also used to describe the influences of feed flow rate, temperature, and ethanol concentration on the membrane performance. This approach is based on solving the conservation equations including continuity and momentum equations that were discretized using finite element method for ethanol in the membrane module. The model was then validated using the experimental data obtained from pervaporation experiments. The simulation results were in good agreement with the experimental data for different values of feed concentration, feed temperature, and Reynolds number (feed flow rate). The CFD results also indicated that as feed temperature and ethanol concentration in the feed solution increased, the ethanol flux enhanced. The feed flow rate was shown to have no significant effect on ethanol flux whereas the feed concentration and temperature had highly significant effects. The developed model is able to predict the mass transport in the feed and membrane sides.

Keywords: Pervaporation; PDMS membrane; Ethanol/water; CFD; Finite element

1. Introduction

Pervaporation (PV) is a separation process, which is based on the selective transport through a dense membrane combined with a phase change of the permeating components from liquid to vapor. PV is recognized as an effective membrane process for separation of azeotropic mixtures, close boiling point mixtures, or isomers [1]. In PV, a mixture of liquids circulates at one surface of a nonporous membrane and the permeate leaves the other side of the membrane as vapor. The mechanism of permeation through PV membranes is that of solution–diffusion [2]. According to the solution–diffusion mechanism, separation in the PV process takes place in two steps: selective sorption of liquid molecules into the membrane surface on the feed side and selective diffusion of them through the membrane due to differences in both of the solubilities and diffusivities of permeating constituents, respectively [3]. The efficiency of PV separation is determined by properties of the target substance and of the membrane, as well as by operation variables such as feed temperature, permeate pressure, feed concentration, and feed flow rate. In order to scale up the experimental results obtained

*Corresponding author.

in the laboratory for industrial applications, certain process parameters need to be optimized and reliable mathematical models are also necessary to predict the influence of the key parameters. Modeling the PV process is important not only for a quantitative understanding of the dependence of fluxes on the process parameters, but is also useful in design calculations for a PV module [4].

Liu et al. [5] applied the computational fluid dynamics (CFD) technique to obtain velocity and concentration distributions in liquid boundary layer of a slit membrane channel. They modeled concentration polarization in a PV membrane module. They found that CFD is a useful tool for the simulation of pervaporative mass transfer in various membrane modules. Also in another research, Liu et al. [6] developed a CFD model to study the effect of concentration polarization in mass transfer process of removing dilute volatile organic compound from water by PV. They examined the effects of baffle on enhancing mass transfer in the module. Their results showed that the average mass transfer coefficient increased with increasing the baffle height.

Rezakazemi et al. [7] developed a mathematical model to study the PV dehydration of water/ethylene glycol mixtures. The CFD model was validated using the experimental data obtained from PV experiments with poly (vinyl alcohol) membrane. They observed that the simulation results are in good agreement with the experimental data for different values of feed flow rates and temperatures.

As understood, there is a definite need for a comprehensive model which can provide a general simulation of separation process in PV. The main objective of the present study is to develop a comprehensive 2D mathematical modeling for prediction permeation behavior of ethanol removal from its aqueous solution by PV process through a commercial polydimethylsiloxane (PDMS)/PVDF/PP composite membrane. The proposed CFD model is a predictive model enables to predict the effects feed flow rate, concentration, and temperature on the performance of hydrophobic PV. For this purpose, the conservation equations including mass and momentum transfer were numerically solved using a finite element method. The effects of key parameters such as feed flow rate, feed ethanol concentration, and feed temperature on the permeation flux are investigated via both the model prediction and the PV experiments.

2. Experimental

The PV apparatus used in the experiments has been previously described in Raisi et al. [8], and Arou-jalian and Raisi [10]. The PDMS/PVDF/PP composite membrane with a functional layer of PDMS (10 mm thickness) used in the experiments was kindly supplied by GKSS Forschungszentrum (Geesthacht, Germany). The membrane was cut into a 15×20 cm piece and held in a flat frame membrane module. Ethanol (99.8%) was purchased from Merck Co. Ltd. (Darmstadt, Germany) and deionized water was used for making aqueous mixtures [8]. The effective surface area of the membrane was 100 cm^2 [9]. The feed flux was 1.53 lit/min. The properties of feed channel are shown in Fig. 1(a).

The total flux (J) and ethanol selectivity (α) were calculated using the following equations, respectively:

$$J = \frac{W}{St} \tag{1}$$

$$\alpha_{EtOH/H_2O} = \frac{Y_{EtOH}/Y_{H_2O}}{X_{EtOH}/X_{H_2O}} \tag{2}$$

where J is the total flux ($kg/m^2 h$), W is the weight of collected permeate (kg), S is the effective membrane surface area (m^2), and t is time duration of the experiment (h). Y_{H_2O} and Y_{EtOH} are the weight fractions of water and alcohol in the permeate, and X_{H_2O} and X_{EtOH} are the weight fractions of water and alcohol in the feed, respectively.

PV experiments were carried out using an apparatus as shown in Fig. 1(b). In PV, the operating parameters have significant effects on the permeate flux and selectivity. In this study, the effect of the feed flow rate which corresponds to Reynolds number (500, 1,000, 1,500, 2,000, 2,200, and 2,500), the feed ethanol concentration (2, 5, 25, 50, 70, and 100 wt.%), and the feed temperature (40, 50, and 60 °C) on the permeation flux was determined by the PV experiments and CFD modeling. All experimental conditions were repeated three times and the average values are reported. The time duration of each experiment was 8 h. The permeate was conducted via a three-way valve into the two series cold-finger condenser traps immersed in liquid nitrogen baths. The collected permeate was weighed and analyzed every one hour.

3. Model development

Fig. 2 demonstrates the model domain used for modeling. The model was proposed for the steady-state ethanol transport through the membranes. The ethanol/water mixture enter at ($y = 0$, feed side) and leave from ($y = L$), and ethanol diffuses through the membrane (x direction) owing to its concentration gradient. In this study, ethanol is separated from the

Fig. 1. (a) Feed channel, (b) Schematic diagram of experimental module for PV.

aqueous feed solution. The driving force for mass transfer across the membrane is accomplished by applying lower partial pressures of the permeants at the permeate side of the membrane than their corresponding equilibrium partial pressure in the feed. The mass transfer of permeants a cross the membrane can be divided into three consecutive steps (10):

- Selective sorption into the membrane at the feed side.
- Selective diffusion through the membrane.
- Desorption into a vapor phase at the permeate side of the membrane.

The conservation equation of mass (continuity) can be used to describe the transfer of ethanol from the feed phase to the permeate side. The differential form of continuity equation for ethanol is [14]:

$$\frac{\partial C_E}{\partial t} + u\nabla C_{\mathrm{E}} = \nabla(-D_{\mathrm{E}}\nabla C_{\mathrm{E}}) + R_{\mathrm{E}} \tag{3}$$

where C_{E} is ethanol concentration, D_{E} is diffusion coefficient, u is velocity vector, and R_{E} is reaction rate of ethanol that in this case is equal zero.

Besides, the momentum equation should be solved to obtain the velocity distribution in the feed side of membrane module. The momentum equation (Navier–Stokes equation) for the proposed system can be written as [14]:

$$\rho\frac{Du}{Dt} = -\nabla P + \mu\nabla^2 u + \rho g \tag{4}$$

The momentum and mass transfer equations should be coupled and solved simultaneously to obtain the concentration distribution of ethanol with the following assumptions:

(1) The solution-diffusion mechanism is assumed to hold true.
(2) The temperature across the membrane thickness is constant.
(3) Steady-state and laminar flow for the feed in the membrane module.
(4) The resistance of the microporous support of the membrane to transport of the penetrants is negligible.
(5) The permeate side of the membrane is dry for the PV under permeate pressure of 1 mm Hg.

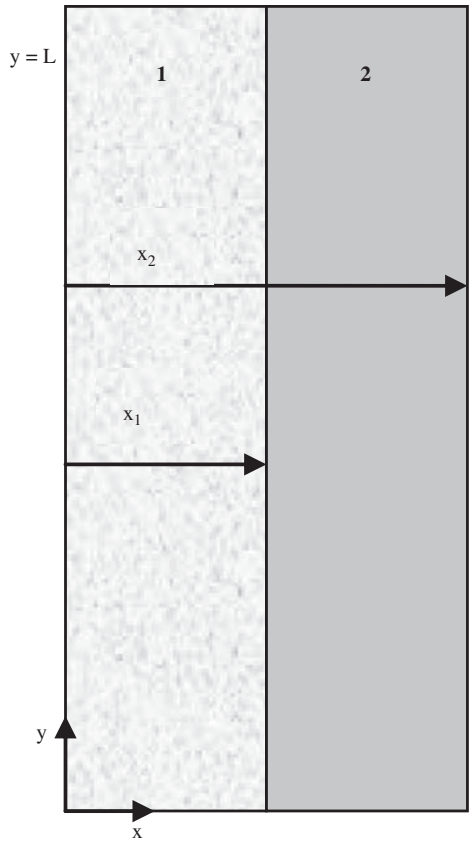

Fig. 2. The model zones and relevant boundaries.

Based on these assumptions, the steady-state continuity equation for the ethanol transport in the feed phase is obtained by simplification of Eq. (3):

$$D_{E,f}\left[\frac{\partial^2 C_{E,f}}{\partial x^2}+\frac{\partial^2 C_{E,f}}{\partial y^2}\right]=u_y\,\frac{\partial C_{E,f}}{\partial y} \tag{5}$$

The boundary conditions for continuity equation in feed side are:

$$\text{At } y=0, \qquad C_{E,f}=C_0 \qquad \text{(inlet concentration)} \tag{6}$$

$$\text{At } y=L, \qquad \frac{\partial C_{E,f}}{\partial y}=0 \qquad \text{(insulation boundary)} \tag{7}$$

$$\text{At } x=0, \qquad \text{(convective flux)} \tag{8}$$

$$\text{At } x=x_1, \qquad C_{E,f}=\frac{C_{E,M}}{m} \tag{9}$$

The convective flux boundary condition assumes that all mass passing through this boundary is convection dominated. This firstly assumes that any mass flux due to diffusion across this boundary is zero. In Eq. (9), m is partition coefficient for ethanol between the feed and the membrane.

For steady-state and laminar flow, Eq. (4) can be simplified as:

$$-\nabla P+\mu\nabla^2 u+\rho g=0 \tag{10}$$

The boundary conditions for Navier–Stokes equation in feed side are:

$$\text{At } x=0,\ p=p_{\text{atm}} \tag{11}$$

$$\text{At } x=x_1,\quad u_y=0 \qquad \text{(No-slip condition)} \tag{12}$$

$$\text{At } y=0,\ u_y=u_0 \qquad \text{(inletvelocity)} \tag{13}$$

$$\text{At } y=L,\quad u_y=0 \qquad \text{(No-slip condition)} \tag{14}$$

The diffusion coefficient of ethanol in water was calculated by the Wilke–Chang [12] equation that applies to diffusion of very dilute i in j:

$$D_{ij}^0=\frac{7.4\times 10^{-8}(\varnothing M_j)^{1/2}T}{\mu_j v_i^{0.6}} \tag{15}$$

where D_{ij}^0 is diffusion coefficient of ethanol in water (cm^2/s), M_j is molecular weight of water, T is temperature (K), μ is viscosity of water (cP), v_i is molar volume of ethanol (mol/cm^3), and $\varnothing$ is an association factor of water that accounts for hydrogen bonding. Then diffusion coefficient was modified with Vignes [16] equation for considering effect of concentration. Vignes [16] proposed that the composition dependence of the diffusivity in a binary ij-mixture be expressed by below relationship:

$$D_{ij}=(D_{ij}^0)^{X_j}(D_{ji}^0)^{X_i} \tag{16}$$

The density of solution was determined by followed equation:

$$\rho_m=\sum \rho_i X_i \tag{17}$$

where ρ_m is the density of solution (kg/m^3), ρ_i is density of each component (ethanol and water) (kg/m^3), and X_i is the weight fractions of each component.

The continuity equation in the membrane can be written as follow:

$$D_{E,M}\left[\frac{\partial^2 C_{E,M}}{\partial x^2}+\frac{\partial^2 C_{E,M}}{\partial y^2}\right]=0 \quad (18)$$

The boundary conditions for the continuity equation in membrane are:

$$\text{At} \quad x=x_1, \quad C_{E,M}=C_{E,f}\times m \quad (19)$$

$$\text{At} \quad x=x_2, \quad C_{E,M}=0 \quad (20)$$

$$\text{At} \quad y=0, \quad \frac{\partial C_{E,M}}{\partial y}=0 \quad \text{(insulation boundary)} \quad (21)$$

$$\text{At} \quad y=L, \quad \frac{\partial C_{E,M}}{\partial y}=0 \quad \text{(insulation boundary)} \quad (22)$$

The use of CFD simulation usually includes three steps: preprocessing, processing, and postprocessing. In the preprocessing step, a specific system is identified. The geometry and material properties should be clearly defined. Meshing usually follows after geometry is determined. This is accomplished by dividing geometry into many small elements or volumes. Meshing is a complicated work, as it is critical for both the accuracy of final result and the cost of numerical calculation. Generally, the finer the divided elements are the closer will be the final solution to the true value at the expense of more calculation time. Much commercial software has its own meshing package. The setting of boundary conditions, initial conditions, and convergence criteria are also completed in the preprocessing stage.

In the processing stage, linear algebraic equation that have been resulted from discritization of the governing equations (continuity and momentum) iteratively calculated in each cell and carried out until convergence criteria are met. This calculation-intensive process constitutes the core content of CFD application.

After the completion of processing, the results can be evaluated either numerically or graphically. The graphical methods provide a more convenient way to evaluate the overall effect. This includes vector plot, contour plot, plot of scalar variables, etc. These visualization tools in postprocessing stage allow quick assessment and comparison of calculation results.

4. Numerical method

The governing equations and constitutive relations are discritized based on the finite element method.

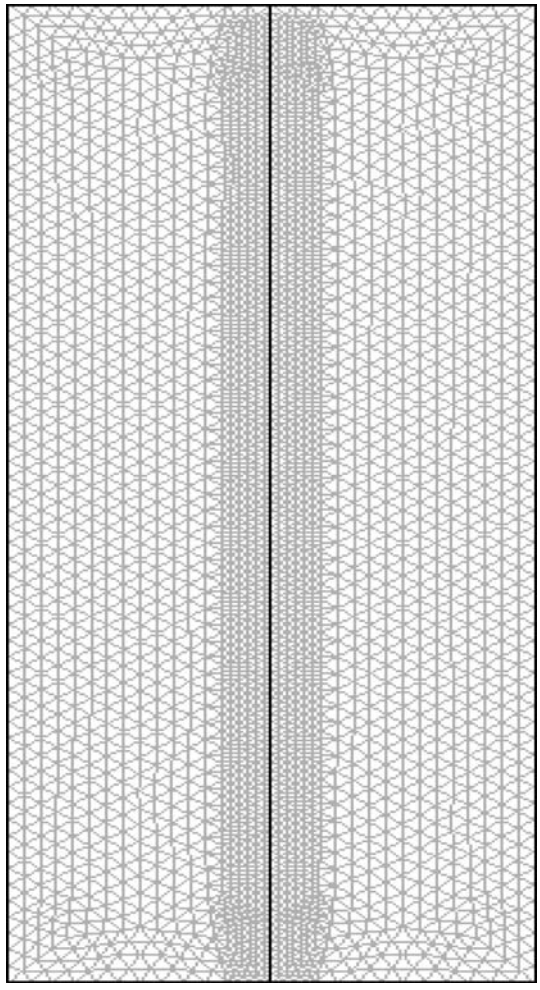

Fig. 3. Magnified segments of the mesh used in the numerical simulation. There are 5,553 elements in total for the whole domain.

The numerical solutions for governing equations were obtained using the COMSOL Multiphysics software version 3.5 [13,15] which applies the finite element analysis with adaptive grid meshing and error controlling by iterative numerical solvers variety. The UMFPACK that is a direct solver is employed for 1D and 2D models [13]. A Mac374YP/A (CPU speed was 1066 MHz and 4 GB of RAM) was used to solve the set of equations. COMSOL generated meshes in triangular shape and in isotropic size. According to grid independency results, 5,553 meshes were applied in the simulation. The computational time for solving the set of equations was about 1 min. Fig. 3 indicates the meshes generated by COMSOL software. Also, Table 1 shows mesh detail and solver parameter used by COMSOL software.

Table 1
Mesh detail and solver parameter used by COMSOL software

Mesh detail		Solver parameter	
No. of degrees of freedom	24,555	Solver	Stationary
No. of mesh points	2,863	Linear system solver	Direct UMFPACK
No. of elements	5,553	Relative tolerance	1×10^{-6}
Mesh shape	Triangular	Maximum no. of iteration	25

5. Results and discussion

5.1. Model validation

The model equations with the boundary conditions were solved in membrane and feed side for ethanol/water mixture at various operating conditions. A comparison between the experimental results and the model predictions was performed.

For better evaluation of the model, ethanol flux was simulated by the model and compared with experimental data. Relative error of the model simulations and the experimental results was calculated by the following formula [11]:

$$\text{Relative error}(\%) = \frac{|J_{\text{Experimental}} - J_{\text{Theoritical}}|}{J_{\text{Experimental}}} \times 100 \qquad (23)$$

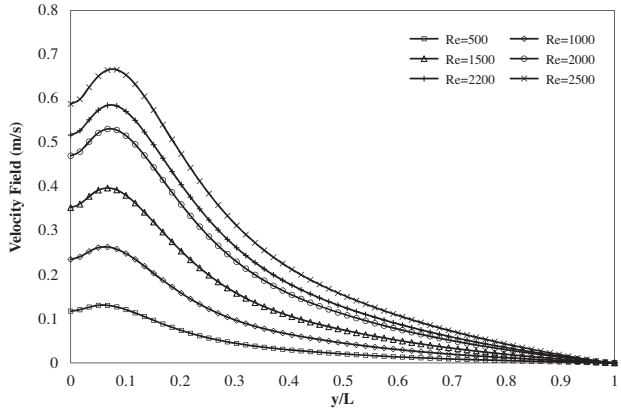

Fig. 4. Velocity profile along the feed side of module at different Reynolds numbers, $T = 40$ ℃, $p = 1$ mmHg, inlet concentration of ethanol = 2 wt.%.

5.2. Velocity distribution

The velocity profile in the feed side of the membrane module was simulated by solving the Navier–Stokes equations. The advantage of solving the Navier–Stokes equation is that the entry effects are considered in the model which can increase the accuracy of the developed model. The velocity profile vs. the dimensionless length (y/L) at different Reynolds numbers in the feed side is shown in Fig. 4. As shown in this figure, there is a maximum in the velocity profile at a region near the entrance on module. The maximum velocity increased with increasing the Reynolds.

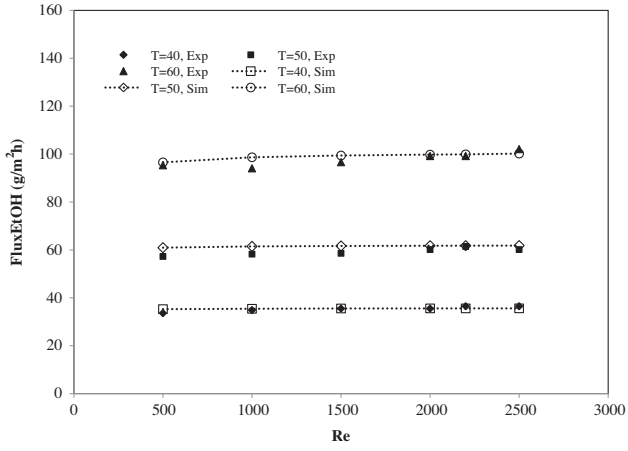

Fig. 5. Experimental and simulation results of the effect of Reynolds number on the ethanol flux at different feed temperatures, $p = 1$ mm Hg, inlet concentration of ethanol = 2 wt%.

5.3. Effect of feed flow rate

Fig. 5 shows the experimental and simulation results of the Reynolds number (feed flow rate) effect on the ethanol flux at different feed temperatures for a 2% ethanol solution under a fixed permeate-side pressure of 1 mmHg. As seen from this figure, the ethanol flux increased slightly when the Reynolds numbers changed from 500 to 2,500 at all feed temperatures. Also, the experimental results confirm the simulation results. It is well known that for the PV process, there is a stagnant liquid boundary layer on the feed side, which leads to a boundary layer resistance for the mass transfer. This is also called concen-

tration polarization phenomena. Increasing the feed flow rate can reduce the boundary layer resistance and increase the mass transfer rate. Therefore, the boundary layer resistance is more important for the case of laminar flow with small Re numbers [17].

5.4. Effect of ethanol feed concentration

Feed concentration has significant effect on both sorption and diffusion phenomena through the membrane. Therefore, the feed concentration is an important variable for the separation properties of PV membranes. The effect of ethanol concentration in the feed on the membrane performance for the separation of ethanol from aqueous solutions by PV at different temperatures was investigated using a PDMS membrane. Fig. 6 shows the ethanol permeation flux vs. ethanol feed concentration in the range of 2–100 wt.% at feed temperatures of 40, 50, and 60˚C.

It can be seen that with increasing the ethanol concentration in feed solution at a given temperature, the ethanol flux increased almost proportionally. This phenomenon could be explained by the solution-diffusion mechanism and in terms of the interaction between the polymer molecules of the hydrophobic PDMS membrane and the ethanol molecules. In binary ethanol/water feed solutions, ethanol is the least polar component. Therefore, an increase in ethanol feed content leads to better swelling of the membrane which results in easier passage of the ethanol molecules through the membrane [19]. Also, an increase in feed ethanol concentration would enhance the driving force of ethanol transfer in the membrane. Moreover, increasing ethanol concentration would also enhance sorption interaction of ethanol in the feed phase with the polymer phase of the membrane. As a result, more ethanol would be found in the membrane phase, which could make the membrane more swelled. Thus, the free volume and chain mobility of the membrane increased, resulting in higher diffusion coefficient of ethanol in the membrane and more ethanol transport through the membrane. Consequently, the ethanol permeation flux increased as the ethanol concentration increased [20]. As indicated in Fig. 6, the experimental results confirm simulation ones.

5.5. Effect of feed temperature

In PV process, feed temperature has a very important role due to its influence on the solubility and the diffusion of the species in the membrane. PV experiments were performed at three different feed temperatures: 40, 50, and 60̊C. The experimental and simulation results in Fig. 7 also show that ethanol permeation flux increased as the feed temperature increased at a given feed concentration. According to the solution-diffusion mechanism [18], component transport through the membrane is achieved by maintaining a lower pressure on the permeate side of the membrane than that on the feed side. When the feed temperature was increased, the difference in vapor pressure across the membrane for the component transport was enhanced. The increased difference in vapor pressure at higher temperatures resulted in an increase in driving force, which helped to increase the permeation flux. In addition, permeating molecules diffuse through free volumes of the membrane. Thermal motions of polymer chains in amorphous regions randomly produce free volumes. As temperature

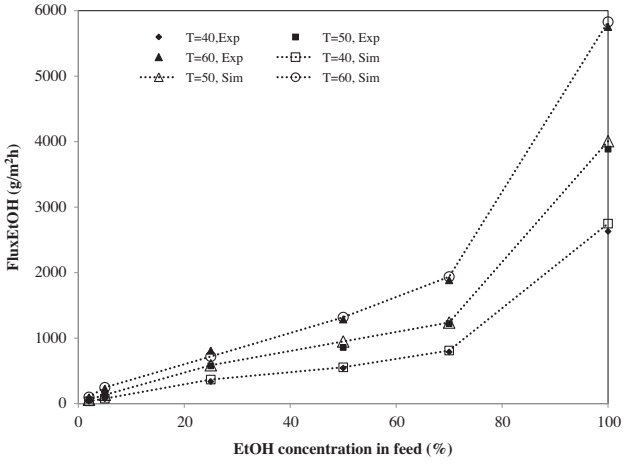

Fig. 6. Experimental and simulation results of the effect of Reynolds number on the ethanol flux at different feed temperatures, $p = 1$ mm Hg, inlet concentration of ethanol = 2 wt.%.

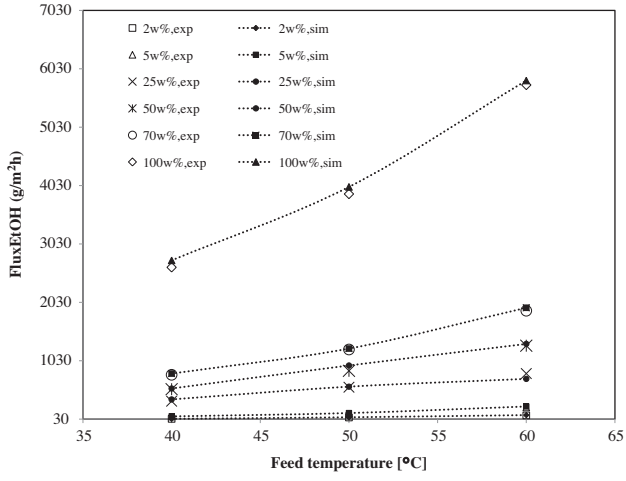

Fig. 7. Experimental and simulation results of the effect of feed temperature on the ethanol flux at different feed concentration, $p = 1$ mm Hg.

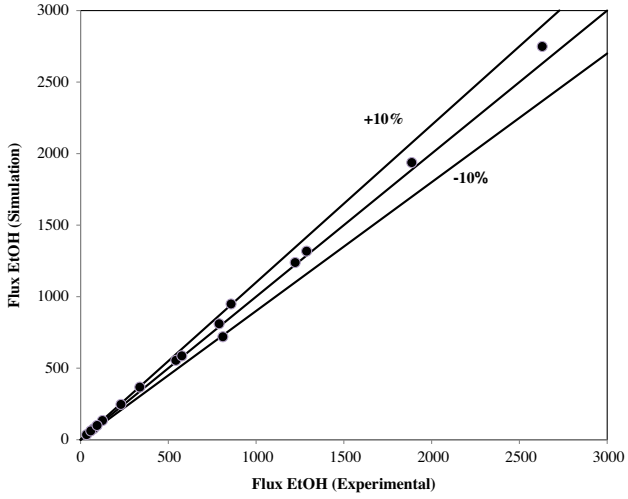

Fig. 8. Parity plot comparing the experimental and simulation results.

increases, frequency and amplitude of polymer jumping chains increase, resulting in an increase in free volume of the membrane. Thus, diffusion rate of individual permeating molecules increases at higher temperatures leading to high permeation fluxes. Another reason for increasing of permeation flux with an increase in feed temperature is that the diffusivity and viscosity of aroma compounds in feed, and the permeability of these compounds into the membrane are affected by the temperature variation in the feed. Thus, feed temperature affects the feed/membrane characteristics and the driving force of process.

A parity plot of comparing between the simulation and experimental results is depicted in Fig. 8. It shows that the simulation results were in good agreement with the experimental ones and the maximum error was around 10%.

6. Conclusions

A general 2D mathematical model was developed to predict the transport of ethanol in the hydrophobic PV with a commercial PDMS membrane. The CFD modeling is based on solving the conservation equations for ethanol in the membrane module. The conservation equations including continuity and momentum equations were derived and solved numerically using the finite element method. The effect of the feed flow rate which is corresponded to Reynolds number, the ethanol feed concentration, and the feed temperature on the permeation flux predicted by the CFD model was investigated and compared with experimental results. The simulation and experimental results showed that the ethanol flux increased as the feed temperature increased. The feed flow rate was shown to have no significant effect on the ethanol flux whereas the feed concentration and temperature had highly significant effects. Finally, it can be said that the model predictions are in good conformity with the experimental results for the ethanol permeation properties, through the PDMS membrane. The proposed CFD model would be helpful to describe the permeation through hydrophobic membranes due to its fully predictive characteristics.

Nomenclature

c	concentration (mol/m^3)
D	diffusion coefficient (m^2/s)
F	body force (N)
J	total flux (kg/m^2.h)
m	partition coefficient
M	molecular weight (kg/mol)
P	pressure (Pa)
s	effective membrane surface area (m^2)
t	PV time (h)
T	temperature (°C)
u	velocity (m/s)
W	permeate weight (kg)
x	x coordinate
y	y coordinate
X	weight fractions in the feed
Y	weight fractions in the permeate
Greek letter	
v	molar volume (cm^3/mol)
μ	viscosity (cp)
ρ	density (kg/m^3)
$\emptyset$	association factor of water
η	dynamic viscosity (kg/m s)
Subscripts/ superscripts	
E	refer to ethanol
E,f	refer to ethanol in feed side
E,m	refer to ethanol in membrane side

References

[1] X. Feng, R.Y.M. Huang, Liquid separation by membrane pervaporation: A review, Ind. Eng. Chem. Res. 36 (1997) 1048.
[2] J. Fontalvo, E. Fourcade, P.C. Cuellar, J.G. Wijers, J.T.F. Keurentjes, Study of the hydrodynamics in a pervaporation module and implications for the design of multi-tubular systems, J. Membr. Sci. 281 (2006) 219–227.
[3] C.K. Yeom, J.C. Jecal, K.H. Lee, Characterization of relaxation phenomena and permeation behaviors in sodium alginate membrane during pervaporation separation of ethanol–water mixture, J. Appl. Polym. Sci. 62 (1996) 1561–1576.
[4] I. Ortiz, D. Gorri, C. Casado, A. Urtiaga, Modelling of the pervaporative flux through hydrophilic membranes, J. Chem. Technol. Biotechnol. 80 (2005) 397–405.

[5] S.X. Liua, M. Peng, L. Vane, CFD modeling of pervaporative mass transfer in the boundary layer, Chem. Eng. Sci. 59 (2004) 5853–5857.
[6] S.X. Liu, M. Peng, L.M. Vane, CFD simulation of effect of baffle on mass transfer in a slit-type pervaporation module, J. Membr. Sci. 265 (2005) 124–136.
[7] M. Rezakazemi, M. Shahverdi, S. Shirazian, T. Mohammadi, A. Pak, CFD simulation of water removal from water/ethylene glycol mixtures by pervaporation, Chem. Eng. J. 168 (2011) 60–67.
[8] A. Raisi, A. Aroujalian, T. Kaghazchi, Experimental study and mass transport modeling of ethanol separation from aqueous solutions by pervaporation, Sep. Sci. Technol. 44 (2009) 3538–3570.
[9] A. Aroujalian, K. Belkacemi, J. Davids, Y. Pouliot, G. Turcotte, Effect of protein on flux and selectivity in pervaporation of ethanol from a dilute solution, Sep. Sci. Technol. 38 (2003) 3239–3247.
[10] A. Aroujalian, A. Raisi, Recovery of volatile aroma components from orange juice by pervaporation, J. Membr. Sci. 303 (1–2) (2007) 154–161.
[11] P. Moradi Shehni, A. Ebadi Amooghin, A. Ghadimi, M. Sadrzadeh, T. Mohammadi, Modeling of unsteady-state permeation of gas mixture through a self-synthesized PDMS membranes, Sep. Purif. Technol. 76 (2011) 385–399.
[12] C.R. Wilke, P. Chang, Correlation of diffusion coefficients in dilute solutions, Am. Inst. Chem. Eng. 1 (1955) 264–270.
[13] M. Keshavarz Moraveji, B. Sajjadi, M. Jafarkhani, R. Davarnejad, Experimental investigation and CFD simulation of turbulence effect on hydrodynamic and mass transfer in a packed bed airlift internal loop reactor, Int. Commun. Heat Mass Transfer 38 (2011) 518–524.
[14] R.B. Bird, W.E. Stewart, E.N. Lightfoot, Transport Phenomena, second ed., Wiley, New York, NY, 2002.
[15] A. Hekmat, A. Ebadi Amooghin, M. Keshavarz Moraveji, CFD simulation of gas–liquid flow behaviour in an air-lift reactor: Determination of the optimum distance of the draft tube, Simul. Modell. Pract. Theory 18 (2010) 927–945.
[16] A. Vignes, Diffusion in binary mixtures, Ind. Eng. Chem. Fundam. 5 (1966) 189–199.
[17] M. She, S.T. Hwang, Concentration of dilute flavor compounds by pervaporation: Permeate pressure effect and boundary layer resistance modeling, J. Membr. Sci. 236 (2004) 193–202.
[18] B. Smitha, D. Suhanya, S. Sridhar, M. Ramakrishna, Separation of organic-organic mixtures by pervaporation: A review, J. Membr. Sci. 241 (2004) 1–21.
[19] M. Garcia, M.T. Sanz, S. Beltrán, Separation by pervaporation of ethanol from aqueous solutions and effect of other components present in fermentation broths, J. Chem. Tech. Biotechnol. 84 (2009) 1873–1882.
[20] Y. Shouliang, Y. Su, Y. Wan, Preparation and characterization of vinyltriethoxysilane (VTES) modified silicalite-1/PDMS hybrid pervaporation membrane and its application in ethanol separation from dilute aqueous solution, J. Membr. Sci. 360 (2010) 341–351.